Published for SISSA by Springer
Received: January 16, 2018
Revised: March 6, 2018
Accepted: March 18, 2018
Published: March 27, 2018

Observation of deconfinement in a cold dense quark medium

V.G. Bornyakov,[b,c] **V.V. Braguta,**[a,b,d,e] **E.-M. Ilgenfritz,**[e] **A.Yu. Kotov,**[a,d,e] **A.V. Molochkov**[b] **and A.A. Nikolaev**[a,b,1]

[a] *Institute for Theoretical and Experimental Physics NRC "Kurchatov Institute", Bolshaya Cheremushkinskaya St. 25, 117218 Moscow, Russia*
[b] *School of Biomedicine, Far Eastern Federal University, Suhanova St. 8, 690950 Vladivostok, Russia*
[c] *Institute for High Energy Physics NRC "Kurchatov Institute", Nauki Sq. 1, 142281 Protvino, Russia*
[d] *Moscow Institute of Physics and Technology, Institutskii per. 9, 141700 Dolgoprudny, Moscow Region, Russia*
[e] *Bogoliubov Laboratory of Theoretical Physics, Joint Institute for Nuclear Research, Joliot-Curie St. 6, 141980 Dubna, Russia*

E-mail: vitaly.bornyakov@ihep.ru, braguta@itep.ru, ilgenfri@theor.jinr.ru, kotov@itep.ru, molochkov.av@dvfu.ru, nikolaev.aa@dvfu.ru

Abstract: In this paper we study the confinement/deconfinement transition in lattice SU(2) QCD at finite quark density and zero temperature. The simulations are performed on an 32^4 lattice with rooted staggered fermions at a lattice spacing $a = 0.044\,\text{fm}$. This small lattice spacing allowed us to reach very large baryon density (up to quark chemical potential $\mu_q > 2000$ MeV) avoiding strong lattice artifacts. In the region $\mu_q \sim 1000$ MeV we observe for the first time the confinement/deconfinement transition which manifests itself in rising of the Polyakov loop and vanishing of the string tension σ. After the deconfinement is achieved at $\mu_q > 1000$ MeV, we observe a monotonous decrease of the spatial string tension σ_s which ends up with σ_s vanishing at $\mu_q > 2000$ MeV. From this observation we draw the conclusion that the confinement/deconfinement transition at finite density and zero temperature is quite different from that at finite temperature and zero density. Our results indicate that in very dense matter the quark-gluon plasma is in essence a weakly interacting gas of quarks and gluons without a magnetic screening mass in the system, sharply different from a quark-gluon plasma at large temperature.

Keywords: Lattice QCD, Phase Diagram of QCD, Quark-Gluon Plasma

ArXiv ePrint: 1711.01869

[1] Corresponding author.

https://doi.org/10.1007/JHEP03(2018)161

JHEP03(2018)161

Contents

JHEP03(2018)161

1 Introduction

The knowledge of the properties of QCD at finite baryon density is very important for understanding cosmology and astrophysics [1, 2]. A thorough experimental study of baryon-rich strongly interacting matter is planned at future heavy ion collision experiments FAIR and NICA. Today, QCD at high energy density and small baryon density is well explored thanks to lattice simulations. Unfortunately, lattice simulations cannot be directly applied to the study of properties of the theory at sufficiently large baryon density because of the sign problem (for a review see, e.g. [3]). For this reason one has a rather poor knowledge about the QCD phase diagram in the region of large baryon density.

There are a lot of phenomenological models which predict different interesting phenomena in this region of the phase diagram. As examples of such phenomena one should mention color flavor locking [4], non-uniform phases in dense matter [5]. More conventional and general features that people believe in are the restoration of chiral symmetry [6] and deconfinement[1] in dense QCD [8] etc. It is rather difficult to estimate systematic uncertainties of different phenomenological models under discussion. So, it is hardly possible to assess if these phenomena are realized in the real world.

In this paper we are going to study the deconfinement aspects of the transition (or transitions) in dense quark matter at low temperature. Since in our consideration it is assumed that the temperature is much smaller than the baryon chemical potential, $T \ll \mu_b$, there is no hope that in the nearest future this region of the phase diagram will be reached by standard methods used to overcome the sign problem in simulations of SU(3) QCD. Instead of considering three-color QCD, in this paper we are going to describe results of lattice simulation of QCD with the SU(2) gauge group. This theory is free from the sign problem and it can be directly studied on the lattice.

SU(2) and SU(3) gauge theories with fundamental quarks have many properties in common. In particular, in both theories confinement/deconfinement and chiral symmetry breaking/restoration transitions take place at a certain non-zero temperature. The

[1]Notice that the confinement/deconfinement and the chiral symmetry breaking/restoration transitions are not immediately related [7], and in dense matter they may take place at different densities.

mechanism of the fermion mass generation in a dense medium and even the formula for the fermion mass gap is the same in both theories [9]. In addition, a lot of (ratios of) observables are almost independent of the number of colors [10].

Still these two theories have some important differences. For instance, the fundamental representation of the SU(2) is pseudoreal, unlike SU(N) with $N \geq 3$, where the fundamental representation is complex. In addition, the chiral symmetry breaking pattern for the SU(3) gauge theory differs from that in the SU(2) theory [11]. In particular, in the SU(2) the chiral symmetry breaking pattern is SU($2N_f$) $\to$ Sp($2N_f$) what differs from the SU(3) where $SU_L(N_f) \times SU_R(N_f) \times U_V(1) \to SU_V(N_f) \times U_V(1)$. So for the SU(2) gauge theory, there is no separate $U_V(1)$ global symmetry whose generator is the baryon number. Instead the generator of the baryon number is a part of the Sp($2N_f$) group. An important consequence of this difference is that SU(2) mesons live in the same representations of Sp($2N_f$) group together with baryons. Notice also that baryons in the SU(2) contain two quarks and they are bosons.

We believe that for both theories at sufficiently large chemical potential or at large temperature the chiral symmetry breaking patterns (which differ in both theories) are not important. Moreover, in these regions of the phase diagram, where the relevant degrees of freedom are quarks and gluons (what happens at large μ or T), it should not be important if baryons are composed of two or three quarks. These arguments make us believe that lattice simulations of the SU(2) gauge theory can be used not only for a qualitative study of dense matter but it can also give quantitative predictions for dense SU(3) QCD.[2]

There are several papers devoted to study of dense lattice SU(2) QCD (see papers [12–15] and references therein). It is clear that — in order to observe deconfinement in dense matter — one needs to reach sufficiently large values of the quark chemical potential without being hampered by lattice artifacts. We believe that the largest values of the quark chemical potential $\mu_q \sim 800 - 1000$ MeV have been safely reached in our previous paper[3] [14]. However, no signatures of the deconfinement phase were observed in the previous paper.

2 Lattice set-up

In the present paper we continue our study of two-color QCD in the region of very large baryon (quark) density. In particular, we carry out lattice simulations with rooted staggered fermions which in the continuum correspond to $N_f = 2$ quark flavours. In order to observe condensation of scalar diquarks in simulation at finite volume we introduced a diquark source term into the lattice action, which is controlled by the parameter λ. In the previous paper [14] we have observed that in the region of large baryon density our results only weakly depend on the value of the parameter λ. In the present paper we have investigated in detail the dependence of the order parameters on λ only for few values of chemical

[2]To prove this statement one needs to conduct numerical simulation the SU(3) theory at nonzero baryon density which is now impossible. So, this statement can be considered as our assumption.

[3]Note that throughout this paper we express our results as functions of the quark chemical potential μ_q. As we study the theory with gauge group SU(2), this corresponds to baryon chemical potential $\mu_b = 2\mu_q$.

JHEP03(2018)161

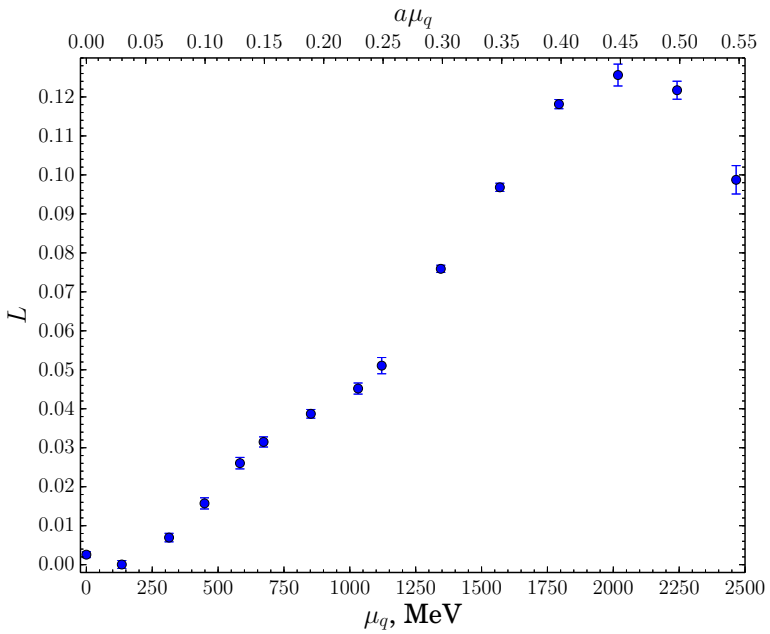

Figure 1. The Polyakov loop $\langle L \rangle$ as a function of the quark chemical potential. The quark chemical potential is shown in physical and lattice units.

potential μ_q and confirmed that the sensitivity is indeed weak. So, in order to reduce the time used for the simulations we restrict our consideration to the value $\lambda = 0.00075$ which is much smaller than the fermion mass $am = 0.0075$ used in the simulations.

Contrary to our previous study we have used now the Symanzik improved gauge action. In addition to the bulk of simulations at finite μ_q, also simulations for calibration at $\mu_q = 0$ have been performed.[4] In this case our string tension at $\mu_q = 0$ amounts to $\sqrt{\sigma_0} = 476(5)$ MeV at $a = 0.044\,\text{fm}$, whereas in our previous study [14] the lattice spacing was almost three times larger, $a = 0.112\,\text{fm}$. This change allowed us to approach the continuum limit much closer and to reach larger baryon densities without being hampered by lattice artifacts. In particular, in the present paper we reach the region of baryon density corresponding to a quark chemical potential $\mu_q > 2000$ MeV which is the largest value ever reached in lattice simulations of SU(2) QCD.

The simulations are performed on a 32^4 lattice (compare with the lattice $16^3 \times 32$ in our previous study [14]). Numerical simulations in the region of large baryon density require considerable computer resources. For this reason, for the present paper we conducted our study at a pion mass of $m_\pi = 740(40)$ MeV, a value which is larger than that used in [14]. We will preferentially decrease the pion mass in our future simulations. In our present study we have $m_\pi L_s \simeq 5$ to be compared with $m_\pi L_s \simeq 3$ in our previous study. In summary, the pion mass is larger but finite volume effects are better under control in the present study.

For the calculation of Wilson loops we have employed one step of HYP smearing [17] for temporal links with the smearing parameters according to the HYP2 parameter set [18],

[4] We used the QCD Sommer scale $r_0 = 0.468(4)\,\text{fm}$ [16] to carry out the scale setting.

JHEP03(2018)161

followed by 24 steps of APE smearing [19] for spatial links only with the smearing parameter $\alpha_{APE} = 0.25$. The same smearing scheme was applied in the paper [20] for the extraction of $V_{Q\bar{Q}}$ from the Wilson loops. In the case of spatial Wilson loops (see below) the smearing scheme was adopted respectively to consider one of the spatial directions as a "temporal direction". For the calculation of the Polyakov loop one step of HYP smearing with the same parameters was employed.

3 Numerical results and discussion

We start the presentation of the results of our study with the measurements of the average Polyakov loop $\langle L \rangle$. The results are shown in figure 1. It is seen from this figure that — contrary to the behaviour of the Polyakov loop at the temperature-driven confinement/deconfinement transition where it is a monotonous function of temperature — the dependence of the Polyakov loop on the chemical potential is rather complicated. First it rises for chemical potential values up to $\mu_q \sim 850$ MeV $(a\mu_q \sim 0.19)$. Then there is a rapid change of the slope in the region $\mu_q \in (850, 1100)$ MeV. From the chemical potential $\mu_q \sim 1100$ MeV $(a\mu_q > 0.25)$, the Polyakov loop rises again reaching a maximum at $\mu_q \sim 2000$ MeV $(a\mu_q \sim 0.45)$, before it drops. It is not quite clear what physical phenomena are hidden behind this highly nontrivial behaviour of the Polyakov loop.

To enquire a possible deconfinement transition in dense matter we measured the interaction potential between a static quark-antiquark pair through the measurement of the Wilson loop. The outcome of this measurement is shown in figure 2. From this figure it is seen that for sufficiently small μ_q the potential $V(r)$ is a linearly rising function of distance, i.e. the system is in the confinement phase. For large values of μ_q the potential $V(r)$ goes to plateau at large distance, i.e. the system is in the deconfinement phase. This allows us to conclude that at large densities the system goes into the deconfinement phase.

Further let us closer determine the chemical potential characterizing the transition from the confinement to the deconfinement phase. To do this we find the string tension σ as a function of the chemical potential through a fit of our data by the Cornell potential $V(r) = \alpha/r + \sigma r + c$. In the fitting procedure we impose the constraint $\sigma \geq 0$. It turns out that at nonzero chemical potential the value of σ depends on the range of distances r covered by the fit. We fit our data in the region $r/a \in [5, 15]$ and account for additional uncertainty due to the variation of the fitting range. The fit is good for not very large values of the chemical potential $\mu_q < 1100$ MeV $(a\mu_q < 0.25)$. For a chemical potential $\mu_q \geq 1100$ MeV the Cornell potential does not describe our data at all.

In figure 3 we plot the ratio σ/σ_0 as a function of the chemical potential, where σ_0 is the string tension at zero chemical potential. One can see from figure 3 that the string tension σ decreases with increasing chemical potential. Thus we see that the system becomes less confined the larger the net quark density is. Finally, in the region $\mu_q \geq 850$ MeV $(a\mu_q \geq 0.19)$ within the uncertainty of the calculation the string tension is zero. So, we conclude that the deconfinement takes place at $\mu_q \geq 850$ MeV.

In order to study how our results are affected by further decreasing the temperature of the system we conducted numerical simulations on the lattice $32^3 \times 48$ with the same

JHEP03(2018)161

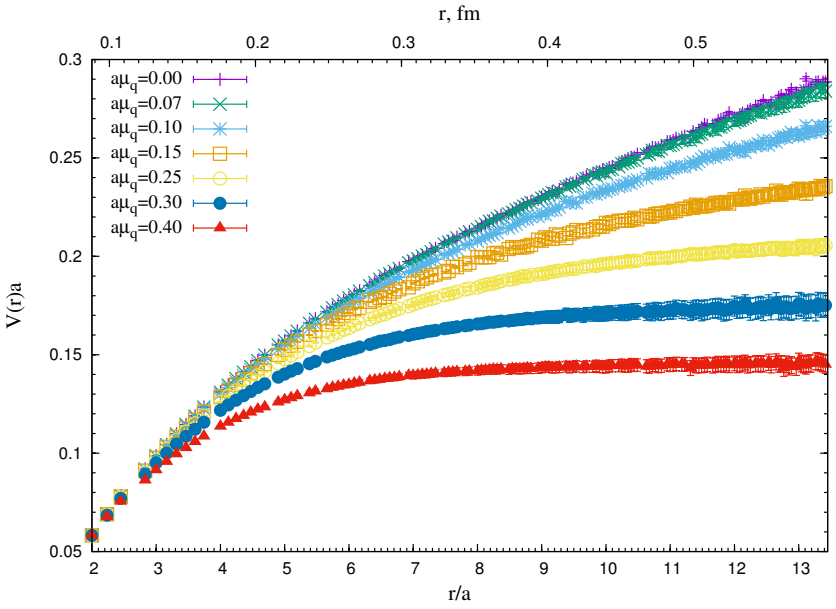

Figure 2. The interaction potential $V(r)$ between a static quark-antiquark pair. The potential is presented in lattice units and the distance between sources is shown in lattice and physical units.

parameters for few values of the chemical potential $a\mu_q = 0.1, 0.2, 0.3, 0.35$. We found that the static potentials obtained in these simulations are equal to those obtained on the lattice 32^4 within the uncertainty of the calculation, but the signal to noise ratio at $N_t = 48$ becomes worse. The respective results in σ/σ_0 are shown in figure 3 with the red triangles. From this study one can conclude that at low temperatures our results concerning confinement/deconfinement transition are not sensitive to the temperature.

As was mentioned above the Cornell potential describes our data quite well at sufficiently small chemical potential and it does not describe the data at large chemical potential. We believe that this happens since at large chemical potential the system under study is in the deconfinement phase where the Cornell potential is not applicable. It is known from $\mu_q = 0$ studies that in the deconfinement phase the static potential of a quark-antiquark pair can be described by the Debye screened potential $V(r) = (\alpha/r)e^{-m_D r} + c$. We fitted our data by a Debye-screened Coulomb potential, the results for Debye mass are shown in figure 4. We found that the fit is good for values $\mu_q \geq 1100$ MeV ($a\mu_q \geq 0.25$), where the screening mass $m_D \neq 0$. In the region $\mu_q < 850$ MeV the Debye potential does not describe our data. Finally, in the region 850 MeV $< \mu <$ 1100 MeV the Debye potential fits data quite well but the m_D equals zero within the uncertainty. Notice that in the region 850 MeV $< \mu <$ 1100 MeV the string tension σ is also zero within the uncertainty of the calculation. This implies that our data do not allow us to distinguish confinement phase from deconfinement phase in this region. So, one can conclude that the confinement/deconfinement transition takes place somewhere in the region $\mu_q \in (850, 1100)$ MeV. Below we will take the midpoint of this interval $\mu_q \sim 1000$ MeV as an estimate of the position of the transition.

JHEP03(2018)161

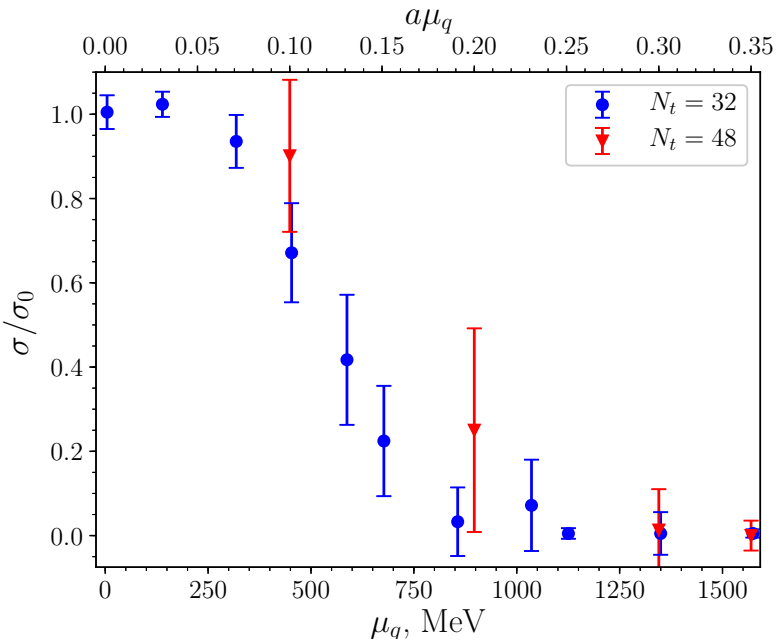

Figure 3. The ratio σ/σ_0 as a function of the quark chemical potential. The constant σ_0 is the string tension at $\mu_q = 0$. The quark chemical potential μ_q is shown in physical and lattice units.

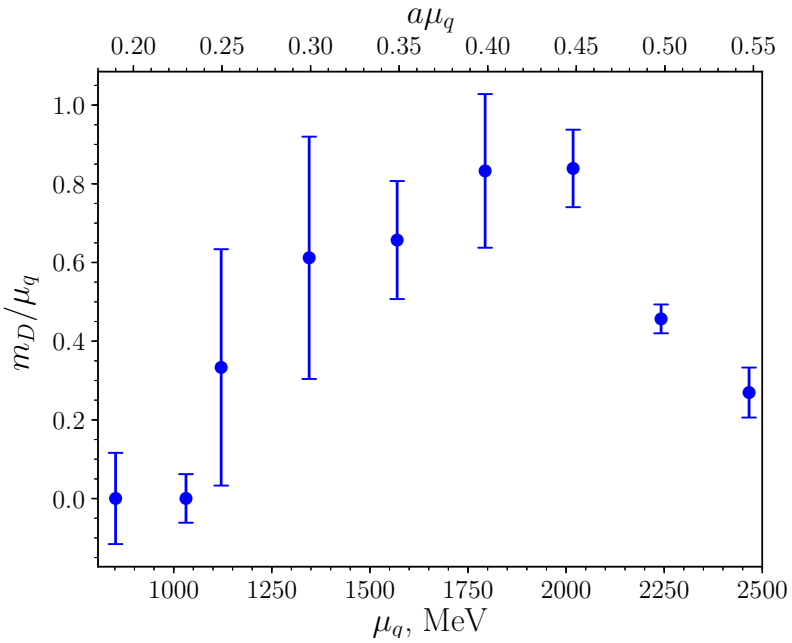

Figure 4. The ratio of Debye mass m_D over the quark chemical potential μ_q as a function of the quark chemical potential, which is shown in physical and lattice units.

JHEP03(2018)161

A more accurate determination of the confinement/deconfinement transition in dense matter might be obtained through the measurement of the susceptibility of the Polyakov loop (as well as other susceptibilities). Unfortunately we are not able to do this since this would require huge statistics which is beyond our presently accessible resources.

To get more insight into the confinement/deconfinement transition in dense matter let us study the dependence of the spatial string tension σ_s on the chemical potential. For this purpose we have measured spacelike Wilson loops. Taking one spatial direction as a "time" direction, one can use the relation between the Wilson loop and the static potential and determine a "spatial potential" $V_s(r)$. To determine the spatial string tension we fit $V_s(r)$ by the Cornell parametrization $V_s(r) = \alpha_s/r + \sigma_s r + c_s$, too. For all values of the chemical potentials under study this form of Cornell potential fits our data well. The fitting parameter σ_s is the spatial string tension. Indeed at large distance the spacelike potential $V_s(r)$ rises as $\sigma_s r$, what implies that the spatial Wilson loop W_s behaves as $W_s \sim \exp(-\sigma_s A)$, where A is a area of the surface spanned by the Wilson loop.

In figure 5 we plot the ratio σ_s/σ_0 as a function of the chemical potential, where σ_0 is the string tension at $\mu_q = 0$. From this figure one recognizes a monotonous decrease of the spatial string tension in the region $\mu_q > 1000$ MeV. Notice that this decrease starts precisely in the region where we have observed the conventional (timelike) confinement/deconfinement transition in our system. The monotonous decrease ends at $\mu_q \sim 2000$ MeV $(a\mu_q \sim 0.45)$ where the spatial string tension has become zero within the uncertainty of the calculation. Thus starting from $\mu_q \sim 2000$ MeV spatial confinement completely disappears. Notice also that in the region $a\mu_q \in (0, 0.1)$ the spatial string tension is smaller than that at zero chemical potential. It is still to be clarified if this is a physical effect or statistical fluctuation.

To understand the physical meaning of this result let us recall that the confinement/deconfinement transition at finite temperature and zero chemical potential is connected with the disappearance of the (conventional, timelike) string tension. On the opposite, above the transition the spatial string tension does not vanish. In contrast, it rises with the temperature, and the spatial potential in QCD has nonzero string tension σ_s at any temperature [21]. This means that there are nonperturbative effects (in the magnetic sector) in zero density QCD for any temperature. From this perspective, the confinement/deconfinement transition at finite density and zero temperature looks quite different. Similarly we observe the vanishing of the string tension. Beyond this net quark (baryonic) density the spatial string tension starts to decrease. Finally, at the chemical potential $\mu_q \sim$ 2000 MeV it also vanishes. Notice that the vanishing of both string tensions indicates the disappearance of all nonperturbative effects in QCD and, in particular, the disappearance of the magnetic screening mass [9]. At the same time, due to asymptotic freedom, the coupling constant is already sufficiently small in the region $\mu_q \geq 2000$ MeV. So, one may conjecture that in the region beyond $\mu_q \sim 2000$ MeV the quark-gluon plasma is essentially a weakly interacting gas of quarks and gluons without magnetic screening mass governing the system.

The picture of the confinement/deconfinement transition in dense matter presented so far in this paper is also supported by our study [22] of Abelian monopoles which are revealed by Abelian projection (in the Maximally Abelian Gauge). It is known that the percolation properties of the Abelian monopoles are related to the temperature-driven

JHEP03(2018)161

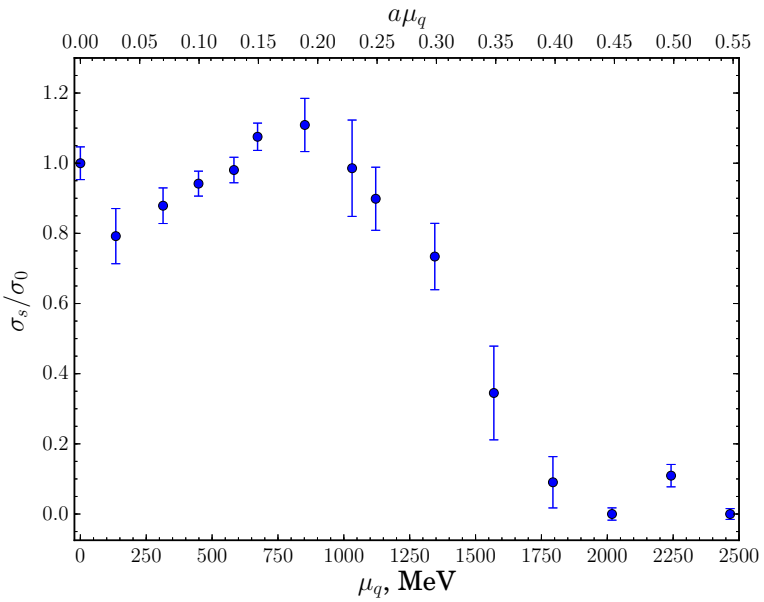

Figure 5. The ratio σ_s/σ_0 (of the spacelike string tension) as a function of the chemical potential. The constant σ_0 is the string tension at $\mu_q = 0$. The quark chemical potential μ_q is shown in physical and lattice units.

confinement/deconfinement transition. In particular, in the confinement phase there is one percolating cluster of monopole currents which disappears at the transition to deconfinement. The same behaviour of the monopole system is accompanying the density-driven confinement/deconfinement transition in dense matter. In our study we observe always a percolating cluster in the confinement phase (at small chemical potential). It disappears at $\mu_q > 1000$ MeV.

It should be added that at high temperature the spatial string tension is related to the density of monopoles trajectories wrapped around the (periodic) temporal extent of the lattice. The larger the density of wrapped monopoles trajectories the larger is the spatial string tension. In our study of dense SU(2) QCD we observe that above the confinement/deconfinement transition at $\mu_q > 1000$ MeV the density of wrapped monopoles trajectories starts to decrease. This behaviour is in agreement with the decrease of the spatial string tension in the same region.

Few words about lattice artifacts are in order. It is known that at large values of the chemical potential $a\mu_q \sim 1$ a saturation effect starts to be seen. The essence of this effect is that all lattice sites are filled with fermionic degrees of freedom, and it is not possible to put more fermions on the lattice ("Pauli blocking"). It is known that the saturation effect is accompanied by the decoupling of the gluons from fermions. Thus, effectively due to saturation, our system becomes gluodynamics which is confined at low temperatures. From this consideration it is clear that — in order to successfully observe deconfinement in dense matter — one should have sufficiently small lattice spacing such that the deconfinement is not spoiled by this kind of artificial confinement at large values of the chemical potential. We believe that for this reason the deconfinement in dense SU(2) matter was not seen before.

JHEP03(2018)161

Now let us return to our results. It may seem from figure 1 that the decrease of the Polyakov loop for $\mu_q > 2000\,\mathrm{MeV}$ might be explained by approaching to the artificial confinement described above. However, we believe that this is not the correct explanation for the following reasons. First, for $\mu_q > 2000\,\mathrm{MeV}$ (up to $\mu_q \sim 2500\,\mathrm{MeV}$) the spatial string tension is vanishing. Second, we do not see a respective rise of the timelike string tension. Moreover, the potential $V(r)$ for $\mu_q > 2000\,\mathrm{MeV}$ is well described by Debye screening potential. So, the properties of the system in the range $\mu_q > 2000\,\mathrm{MeV}$ are very different from those of plain gluodynamics at small temperatures. For this reason we believe that in the region under consideration in this work, $\mu_q < 2500\,\mathrm{MeV}$ ($a\mu_q \leq 0.55$) our results are not spoiled by eventual saturation effects.

The results of this paper lead us to conclude that the confinement/deconfinement transition takes place at $\mu_q \sim 1000$ MeV. A more detailed study of the position of the transition, extending this study to more realistic pion masses, will be the goal of our forthcoming study.

Our study of the confinement/deconfinement transition was only possible in lattice SU(2) QCD. At the end of this paper let us discuss the applicability of our results for the case of SU(3) QCD. As was noted above there are two very important differences between two-color and three-color QCD. The first one is that the chiral symmetry breaking pattern of the two theories is different. The second one is that baryons in the SU(3) theory are fermions and contain three quarks whereas in the SU(2) theory baryons are bosons and contain two quarks. According to our results the confinement/deconfinement transition takes place at very large baryon density ($\mu_q \sim 1000$ MeV). Notice that in this region of μ_q the chiral symmetry is already restored [14]. So, we believe that the chiral symmetry breaking pattern does not play any role in this region. Moreover, according to our previous results [14] in the region of large baryon density the key degrees of freedom are quarks rather than baryons. Notice also that the ratios of the critical temperature of the confinement/deconfinement transitions to the string tension $T_c/\sqrt{\sigma_0}$ in two-color and three-color QCD are close to each other. These facts allow us to conjecture that if the mechanism of the deconfinement in the cold dense matter is the same in SU(2) and SU(3) theories the confinement/deconfinement transition in SU(3) theory takes place in the region $\mu_q/\sqrt{\sigma_0} \sim 2.1$. We can also conjecture that the physical scenario of the transition in the SU(3) theory is similar to that in the SU(2) case. In particular, we expect that the vanishing of the string tension is followed by the vanishing of the spatial string tension at sufficiently large baryon density also in SU(3) QCD.

4 Conclusion

In conclusion, in this paper we have studied the confinement/deconfinement transition aspects in dense lattice SU(2) QCD. The simulations were performed on a space-time symmetric lattice 32^4 with rooted staggered fermions at lattice spacing $a = 0.044\,\mathrm{fm}$. The small lattice spacing has allowed us to reach the region of very large baryon density ($\mu_q > 2000$ MeV) without getting results spoiled by lattice artifacts. We have measured the Polyakov loop, the interaction potential between static quark-antiquark pair, the string tension and the spatial string tension for different values of the quark chemical potential.

JHEP03(2018)161

In the region $\mu_q \sim 1000$ MeV we have observed the confinement/deconfinement transition which manifests itself in rising of the Polyakov loop and vanishing of the string tension. After the onset of deconfinement $\mu_q > 1000$ MeV we have observed a monotonous decrease of the spatial string tension which ends with the vanishing of this observable in the region $\mu_q > 2000$ MeV. Thus, the confinement/deconfinement transition at finite density and zero temperature is quite different from that at finite temperature and zero density. In addition one may expect that in very dense matter the quark-gluon plasma becomes a weakly interacting gas of quarks and gluons without magnetic screening mass in the system, much different from the quark-gluon plasma at large temperature.

Acknowledgments

V.V.B. acknowledges the support from BASIS foundation. The work was partially supported by RFBR grant 16-32-00048. The work of A.V.M. was carried out within the state assignment of the Ministry of Science and Education of Russia (Grant No. 3.6261.2017/8.9). The work of V.G.B was supported by RFBR grant 16-02-01146. This work has been carried out using computing resources of the federal collective usage center Complex for Simulation and Data Processing for Mega-science Facilities at NRC "Kurchatov Institute", http://ckp.nrcki.ru/. In addition, we used the supercomputer of the Institute for Theoretical and Experimental Physics (ITEP).

References

[1] J.M. Lattimer and M. Prakash, *The equation of state of hot, dense matter and neutron stars*, *Phys. Rept.* **621** (2016) 127 [arXiv:1512.07820] [INSPIRE].

[2] N. Itoh, *Hydrostatic equilibrium of hypothetical quark stars*, *Prog. Theor. Phys.* **44** (1970) 291 [INSPIRE].

[3] S. Muroya, A. Nakamura, C. Nonaka and T. Takaishi, *Lattice QCD at finite density: an introductory review*, *Prog. Theor. Phys.* **110** (2003) 615 [hep-lat/0306031] [INSPIRE].

[4] M.G. Alford, K. Rajagopal and F. Wilczek, *Color flavor locking and chiral symmetry breaking in high density QCD*, *Nucl. Phys.* **B 537** (1999) 443 [hep-ph/9804403] [INSPIRE].

[5] T. Kojo, Y. Hidaka, L. McLerran and R.D. Pisarski, *Quarkyonic chiral spirals*, *Nucl. Phys.* **A 843** (2010) 37 [arXiv:0912.3800] [INSPIRE].

[6] M.G. Alford, K. Rajagopal and F. Wilczek, *QCD at finite baryon density: nucleon droplets and color superconductivity*, *Phys. Lett.* **B 422** (1998) 247 [hep-ph/9711395] [INSPIRE].

[7] H. Suganuma, T.M. Doi, K. Redlich and C. Sasaki, *Relating quark confinement and chiral symmetry breaking in QCD*, *J. Phys.* **G 44** (2017) 124001 [arXiv:1709.05981] [INSPIRE].

[8] L. McLerran and R.D. Pisarski, *Phases of cold, dense quarks at large N_c*, *Nucl. Phys.* **A 796** (2007) 83 [arXiv:0706.2191] [INSPIRE].

JHEP03(2018)161

[9] D.T. Son, *Superconductivity by long range color magnetic interaction in high density quark matter*, *Phys. Rev.* **D 59** (1999) 094019 [hep-ph/9812287] [INSPIRE].

[10] B. Lucini and M. Panero, SU(N) *gauge theories at large* N, *Phys. Rept.* **526** (2013) 93 [arXiv:1210.4997] [INSPIRE].

[11] J.B. Kogut, M.A. Stephanov, D. Toublan, J.J.M. Verbaarschot and A. Zhitnitsky, *QCD-like theories at finite baryon density*, *Nucl. Phys.* **B 582** (2000) 477 [hep-ph/0001171] [INSPIRE].

[12] J.B. Kogut, D. Toublan and D.K. Sinclair, *The phase diagram of four flavor* SU(2) *lattice gauge theory at nonzero chemical potential and temperature*, *Nucl. Phys.* **B 642** (2002) 181 [hep-lat/0205019] [INSPIRE].

[13] S. Cotter, P. Giudice, S. Hands and J.-I. Skullerud, *Towards the phase diagram of dense two-color matter*, *Phys. Rev.* **D 87** (2013) 034507 [arXiv:1210.4496] [INSPIRE].

[14] V.V. Braguta, E.M. Ilgenfritz, A. Yu. Kotov, A.V. Molochkov and A.A. Nikolaev, *Study of the phase diagram of dense two-color QCD within lattice simulation*, *Phys. Rev.* **D 94** (2016) 114510 [arXiv:1605.04090] [INSPIRE].

[15] L. Holicki, J. Wilhelm, D. Smith, B. Wellegehausen and L. von Smekal, *Two-colour QCD at finite density with two flavours of staggered quarks*, PoS(LATTICE2016)052 [arXiv:1701.04664] [INSPIRE].

[16] A. Bazavov et al., *The chiral and deconfinement aspects of the QCD transition*, *Phys. Rev.* **D 85** (2012) 054503 [arXiv:1111.1710] [INSPIRE].

[17] A. Hasenfratz and F. Knechtli, *Flavor symmetry and the static potential with hypercubic blocking*, *Phys. Rev.* **D 64** (2001) 034504 [hep-lat/0103029] [INSPIRE].

[18] M. Della Morte, A. Shindler and R. Sommer, *On lattice actions for static quarks*, *JHEP* **08** (2005) 051 [hep-lat/0506008] [INSPIRE].

[19] APE collaboration, M. Albanese et al., *Glueball masses and string tension in lattice QCD*, *Phys. Lett.* **B 192** (1987) 163 [INSPIRE].

[20] C. Bonati, M. D'Elia, M. Mariti, M. Mesiti, F. Negro and F. Sanfilippo, *Anisotropy of the quark-antiquark potential in a magnetic field*, *Phys. Rev.* **D 89** (2014) 114502 [arXiv:1403.6094] [INSPIRE].

[21] M. Cheng et al., *The spatial string tension and dimensional reduction in QCD*, *Phys. Rev.* **D 78** (2008) 034506 [arXiv:0806.3264] [INSPIRE].

[22] V.G. Bornyakov et al., to be published.

JHEP03(2018)161